www.czasopisma.pan.pl PAN www.journals.pan.pl
Chemical and Process Engineering 2018, 39 (2), 233–246
DOI: 10.24425/122946

ACETONE ADSORPTION ON CO_2-ACTIVATED TYRE PYROLYSIS CHAR – THERMOGRAVIMETRIC ANALYSIS

Tomasz Kotkowski, Robert Cherbański*, Eugeniusz Molga

Warsaw University of Technology, Faculty of Chemical and Process Engineering,
ul. Waryńskiego 1, 00-645 Warsaw, Poland

Activation of tyre pyrolysis char (TPC) can significantly increase its market value. To date, it has been frequently carried out in different reactors. In this work, thermogravimetric analysis was used instead. The performance of activated pyrolysis chars was tested by adsorption of acetone vapour and comparison of the equilibrium adsorption capacities for all samples. The highest equilibrium adsorption capacity was observed for the carbon burn-off of $\sim 60\%$. In addition, the equilibrium adsorption capacity of activated TPC decreases by about 10% after eleven adsorption/desorption cycles. Moreover, activation changed the porous structure of pyrolysis chars from mesoporous to micro-mesoporous.

Keywords: physical activation, char, end-of-life tyres, pyrolysis, TGA

1. INTRODUCTION

Used tires can be divided into two groups: part-worn tyres and end-of-life-tyres (ELTs). The difference between part-worn tyres and ELTs is that the former can be reused whereas the latter cannot be used on vehicles anymore. To decrease their negative environmental impact ELTs should be reprocessed. In the EU, the total mass of generated ELTs was 2.63 million tonnes in 2013 (ETRMA, 2015).

Because of potential hazards associated with landfilling and stockpiles of ELTs (landfill fires with emissions of toxic gases, contamination of surface and groundwater and health risks), the direct disposal of ELTs in landfills is banned in the EU. Therefore, the management of ELTs is organised in the form of material recovery and energy recovery. Tyre pyrolysis is an attractive form of material recovery in which char, oil, gas and metal are produced. Estimated yields of the end-products are: 33% char, 35% oil, 20% gas and 12% metal (Sharma, 1998). The gas and oil can be directly used to heat the pyrolysis reactor. Oil can also be distilled to recover certain chemical compounds such as: benzene, toluene, xylenes and limonene. On the other hand, the char needs to be activated to obtain the secondary product of relatively high market value.

An overview of studies on the activation of TPC can be found in the excellent review by Antoniou et al. (2014). The review presents the state-of-the-art till 2014. Since then, several new articles have been published on the topic.

Antoniou and Zabaniotou (2015) reported on the experimental investigation and technical assessment of ELT pyrolysis in a batch rotary kiln reactor. They examined the effect of temperature, heating rate and particle size on product yields. Chemical activation of pyrolysis char with KOH resulted in the BET

* Corresponding author, e-mail: Robert.Cherbanski@pw.edu.pl

surface area of 402 m^2/g. In their recent paper (Antoniou and Zabaniotou, 2018), a pyrolysis prototype was designed, constructed, and demonstrated at Technology Readiness Level 7. As part of the project, valorisation of the char was also carried out. The TPC was activated with steam and KOH showing the BET surface area of 589 m^2/g and 402 m^2/g, respectively.

Acevedo and Barriocanal (2015) obtained activated carbons from tyre wastes and their blends with coal and a bituminous waste material. Carbon dioxide was used as an activating agent. The BET surface area of activated carbons produced from the tyre wastes was in the range of 390 and 475 m^2/g. The activated carbons had a mesoporous structure. The BET surface area of the blends was much higher due to developed microporosity and reached 1120 m^2/g.

Hadi et al. (2016) produced mesoporous activated carbon from TPC using steam as an activating agent. The effect of activation temperature and residence time was tested. The BET surface area and total pore volume increased as a result of activation from 32 to 732 m^2/g and from 0.18 to 0.91 cm^3/g, respectively. In addition, the BET surface area, mesopore volume and total pore volume increased linearly with burn-off during activation.

Acosta et al. (2016) prepared activated carbons from TPC by KOH activation. The weight ratios of KOH to TPC were between 0.5 and 6, while the activation temperatures were in the range of 600 to 800 °C. The maximum BET surface area of 814 m^2/g was reported for the activation temperature of 750 °C and the weight ratio of 6. As a compromise between the BET surface areas, yields and the weight ratios, activated carbon having 700 m^2/g was finally chosen for sorption of tetracycline from aqueous phase. Its performance was similar to commercial activated carbon (CAC). In addition, a successful removal of Bisphenol A from aqueous solutions was recently demonstrated using the same activated TPC (Acosta et al., 2018). This activated TPC showed to be better than CAC recommended for BPA adsorption.

Seng-eiad and Jitkarnka (2016) studied the possibility of using untreated and 5 M HNO_3-treated chars as catalysts for waste tire pyrolysis. A thorough characteristic of both chars was an important aspect of this work. The treatment of TPC with nitric acid resulted in the increase of the BET surface area from 70.06 to 96.10 m^2/g with practically unchanged mesoporous internal structure.

Farooq et al. (2018) investigated the effect of waste tire (WT) addition to wheat straw (WS) pyrolysis feedstock on the yield, quality and quantity of pyrolysis oil. Samples of WT, WT and their different blends were pyrolysed showing the synergistic effects of co-pyrolysis technique for a WS/WT 2:3 feedstock.

Han et al. (2018) investigated the mechanism of waste tyre pyrolysis by the coupled thermogravimetry and mass spectrometry techniques. The surface functional groups on TPC were characterised using Fourier Transform Infrared Spectroscopy. Four stages were distinguished in the course of pyrolysis.

Thermogravimetric analysis (TGA) is a well-established method of thermal analysis. TGA is carried out in a thermobalance. The measuring principle is based on an accurate measurement of sample mass as a function of temperature or time in a strictly defined and controlled gas atmosphere. TGA can characterise materials that exhibit weight loss or gain. Thus, this technique is very helpful in studying adsorption/desorption processes in various systems (Cortes et al., 2010; Kruk et al., 2001; Lin et al., 2006; Majchrzak-Kucęba and Nowak, 2005; Muller et al., 1998). In addition, the following processes can be investigated using TGA: evapouration, reduction, decomposition, absorption. TGA is also frequently used for controlling a material's thermal stability and composition.

The aim of this paper is to investigate adsorptive properties of CO_2-activated TPC. These properties are examined using two different methods: TGA and nitrogen adsorption at 77 K. TGA is employed to activate TPC and to test the equilibrium adsorption capacity of the activated TPC with acetone. In turn, nitrogen adsorption at 77 K is used to measure the BET surface areas and pore size distributions of the activated

TPCs. As far as we know these complementary approaches have been used for the first time to examine adsorptive properties of the activated TPCs. As mentioned above, previous papers dealt with activation of TPC carried out in different reactors, such as rotary kilns, multiple hearths and fluidised beds (Antoniou et al., 2014).

2. MATERIALS AND METHODS

2.1. Materials

Granular activated carbon (GAC), purchased from Chempur (Poland), was the reference adsorbent. Its physico-chemical properties are listed in Table 1.

Table 1. Physico-chemical properties of GAC

Parameter	Value
Shape	cylindrical
Diameter	approx. 1 mm
Length	approx. 4 mm
Bulk density	454 g/dm^3
Mechanical strength	95.9%
Abrasion resistance	0.18%
Moisture content	2.1%
Methylene blue number	25 cm^3
Iodine number	997 mg/g
Water absorbability	0.88 cm^3/g
pH of water extract	10.4

Shredded ELTs of different types were used for production of pyrolysis char in a pyrolysis pilot plant (see the next subsection for details). ELTs were pretreated to remove steel cords.

Acetone (CAS: 67-64-1; purity $\geq$ 99.5%), purchased from Chempur (Poland), was used as the adsorbate. Nitrogen (purity $\geq$ 99.999%), carbon dioxide (purity $\geq$ 99.99%) and synthetic air (purity $\geq$ 99.999%), delivered by Multax (Poland) were used as purge gases in TGA. Nitrogen was also used as the protective gas. Gas impurities are listed in Table 2.

Table 2. Gas impurities

Impurites	N_2 (ppm)	CO_2 (ppm)	Air (ppm)
H_2O	< 3	< 10	< 3
O_2	< 2	< 10	–
C_nH_m	< 0.1	–	< 0.1
CO	< 0.1	–	< 0.1
CO_2	< 0.5	–	< 0.5
H_2	< 1	–	< 1

2.2. Production of pyrolysis char

Figure 1 presents a schematic diagram of the pyrolysis pilot plant. The pyrolysis pilot plant was designed and built at our home university to perform thorough and extensive investigations of ELT pyrolysis and to formulate guidelines for a full-scale pyrolysis plant. The pyrolysis pilot plant comprises a batch tank reactor equipped with a low-speed scraping stirrer (10 rpm), a two-section condenser, a pyrolysis oil tank (being also a gas-liquid separator), and a non-condensing pyrolysis gas burner. The diameter and length of the reactor chamber are 0.31 and 1.06 m, respectively. Its working volume is approx. 75 dm^3. The pyrolysis reactor was heated using a 7.4 kW electric heater. The pyrolysis char investigated in this work was produced at 500 °C.

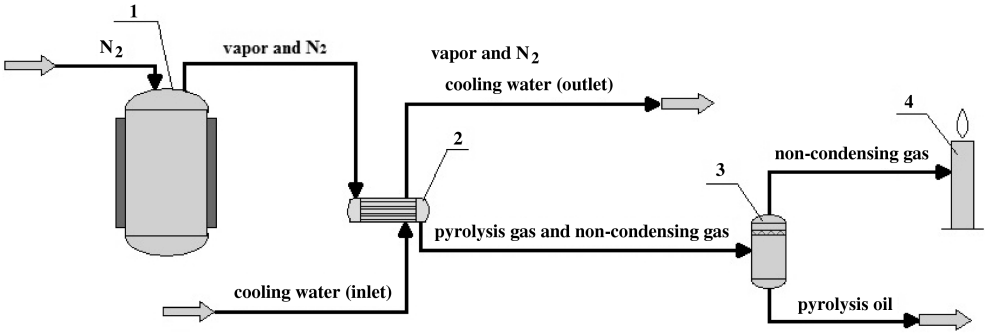

Fig. 1. Schematic diagram of the pyrolysis pilot plant from which the TPC was collected. (1) Pyrolysis reactor with shredded ELTs, (2) two-section condenser, (3) oil tank (gas-liquid separator), (4) gas burner

2.3. Thermogravimetric analysis

Fig. 2 shows a schematic diagram of the experimental setup for TGA experiments.

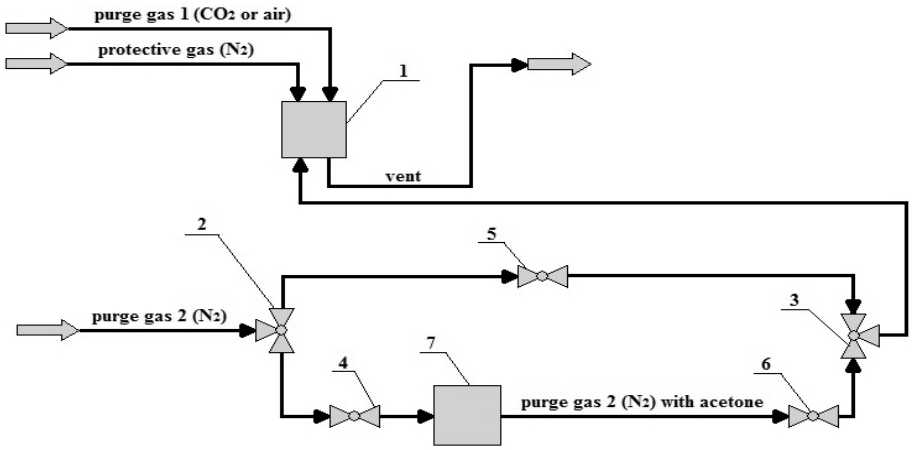

Fig. 2. Schematic diagram of the experimental setup for TGA experiments. (1) Thermobalance, (2–3) three-way valve, (4–6) valve, (7) thermostated bubbling washer with acetone

TGA was carried out in the TG 209 F1 Libra thermobalance (Netzsch, Germany). The thermobalance contains a ceramic micro furnace and a precise micro balance. The micro furnace can heat a sample to the maximum temperature of 1100 K. The heating rates of the micro furnace are in the range of 0.001–200 K/min. The micro balance under thermostatic control provides resolution of 0.1 μg. The thermobalance is equipped with three mass flow controllers to regulate the flow of two purge gases and one protective gas. The crucibles with a volume of 300 μl and a sample carrier type P with protected thermocouple and radiation shield made of Al_2O_3 were used in all experiments.

Table 3 presents conditions of all performed TGA experiments. Measurements No. 1 and 2 were aimed at investigating the equilibrium adsorption capacity of the degassed GAC and TPC.

Table 3. Conditions of the performed TGA. Measurement No. 10 – eleven cycles performed. * Abbreviations used: H – heating, I – isothermal, C – cooling, Ace (N_2) – acetone vapour carried by nitrogen

Run No.	Name	Material	Stage*	Initial temp. (°C)	Heating rate (°C/min)	Final temp. (°C)	Duration of the isotherm. stage (min)	Gas*	Volum. flow rate (ml/min)
1	GAC_Des(200)_Ads(25)	GAC	H	25	50	200	–	N_2	100
			I	200	0	200	15	N_2	
			C	200	40	100	–	N_2	
			C	100	10	25	–	N_2	
			I	25	0	25	120	Ace (N_2)	
2	Char_Des(500)_Ads(25)	char	H	25	50	500	–	N_2	100
			I	500	0	500	15	N_2	
			C	500	40	100	–	N_2	
			C	100	10	25	–	N_2	
			I	25	0	25	120	Ace (N_2)	
3	Char_Comb(800)	char	H	25	50	800	–	Air	100
			I	800	0	800	60	Air	
4	Char_A(900)_Ads(25)	char	H	25	50	900	–	CO_2	100
			I	900	0	900	85	CO_2	
			C	900	40	100	–	N_2	
			C	100	10	25	–	N_2	
			I	25	0	25	120	Ace (N_2)	
5	Char_A(950)_Ads(25)	char	H	25	50	950	–	CO_2	100
			I	950	0	950	85	CO_2	
			C	950	40	100	–	N_2	
			C	100	10	25	–	N_2	
			I	25	0	25	120	Ace (N_2)	
6	Char_A(1000)_Ads(25)	char	H	25	50	1000	–	CO_2	100
			I	1000	0	1000	85	CO_2	
			C	1000	40	100	–	N_2	
			C	100	10	25	–	N_2	
			I	25	0	25	120	Ace (N_2)	
7	Char_A(1050)_Ads(25)	char	H	25	50	1050	–	CO_2	100
			I	1050	0	1050	85	CO_2	
			C	1050	40	100	–	N_2	
			C	100	10	25	–	N_2	
			I	25	0	25	120	Ace (N_2)	
8	Char_A(1100)_Ads(25)	char	H	25	50	1100	–	CO_2	100
			I	1100	0	1100	85	CO_2	
			C	1100	40	100	–	N_2	
			C	100	10	25	–	N_2	
			I	25	0	25	120	Ace (N_2)	
9	Char_A(1110)_Ads(25)	char	H	25	50	1110	–	CO_2	100
			I	1110	0	1110	110	CO_2	
			C	1110	40	100	–	N_2	
			C	100	10	25	–	N_2	
			I	25	0	25	120	Ace (N_2)	
10	Char_A(1000)_CyclesAdsDes	char	H	25	50	200	–	N_2	100
			I	200	0	200	5	N_2	
			C	200	40	100	–	N_2	
			C	100	10	25	–	N_2	
			I	25	0	25	85	Ace (N_2)	

Measurement No. 3 was performed to find the ash content of TPC. In measurements No. 4–9, the effect of temperature on activation of TPC was investigated and adsorption of acetone vapour on the activated char was carried out. Measurement No. 10 was carried out to check a possible change in the equilibrium adsorption capacity after eleven adsorption/desorption cycles.

Acetone vapour was introduced into the thermobalance chamber by nitrogen, being the carrier gas that flowed through a bubbling washer with acetone. To avoid vapour condensation the bubbling washer was thermostated at 18 °C (below the room temperature). Acetone was chosen as a representative of VOCs to be used in our experiments. Acetone has high relative vapour pressure at approximately room temperature which effects in the relatively high equilibrium adsorption capacity as follows from any adsorption isotherm. Note that the equilibrium adsorption capacity is related to the mass gain measured in the thermobalance. This mass gain is significant for acetone.

2.4. Surface characterisation

The 3Flex Surface Characterization Analyzer (Micromeritics, USA) was used to examine the surface characteristics of GAC, non-activated and activated pyrolysis chars. All calculations were carried out on the basis of the nitrogen adsorption/desorption isotherms determined at −196 °C. Prior to main measurements, samples of about 100–200 mg were degassed under vacuum (1 mmHg) using a two-stage temperature program: (1) 90 °C for 1 h, and (2) 300 °C for 15 h (Smart VacPrep, Micromeritics, USA). Degassing was necessary to clean the internal surface from moisture and other gases. The BET surface area was calculated from a BET plot in the relative pressure range between 0.0089 and 0.058. The micropore surface area was calculated using the t-plot method. Porosity distribution was calculated using the Non-Local-Density-Functional Theory (NLDFT). The N2-DFT model was employed in calculations assuming a slit-like pore geometry with the pore size range covered from 4.0 to 4000 Å.

3. RESULTS AND DISCUSSION

Combustion of pyrolysis char in synthetic air (Run No. 3, Table 3) is presented in Fig. 3. Note that two measurements were carried out giving the same results. They were performed by heating the samples at a constant heating rate up to the final temperature of 800 °C followed by an isothermal step. One measurement was performed in a classical way with a baseline correction, whereas the other was conducted without the baseline run. Instead, the BeFlat®mode, patented by Netzsch, was used. The BeFlat®mode automatically compensates for the change in buoyancy caused by temperature changes. Since the two resulting curves overlap, the BeFlat®mode has been used in successive measurements. In addition, these experiments show that the ash content in the pyrolysis char is 19.39 wt%. The ash content depends on tyre manufacture. Therefore, it is different for passenger car, truck and motorcycle tyres. It also depends on the tyre brand. This is the reason why the ash content is reported in the literature in very wide limits, i.e. from 7.7 to 40.80 wt% (Martinez et al., 2013). Moreover, as follows from Figure 3, the amount of moisture and volatiles is rather low (0.70 wt%) when compared to previous results reported in the literature: 0.00–3.57 wt% for the moisture content and 0.67–16.14 wt% for volatiles (Martinez et al., 2013; Williams, 2013). We believe that our result is due to the experimental methodology applied in our pyrolysis pilot plant which is briefly explained below. The pyrolysis char was discharged from the pyrolysis reactor after it had cooled down, i.e. after about 24 hours. Then, it was stored in a closed vessel. Note that the pyrolysis reactor was flushed with nitrogen during cooling of the reactor. As a result, the pyrolysis char was subjected to high temperature for a long time after the pyrolysis was completed.

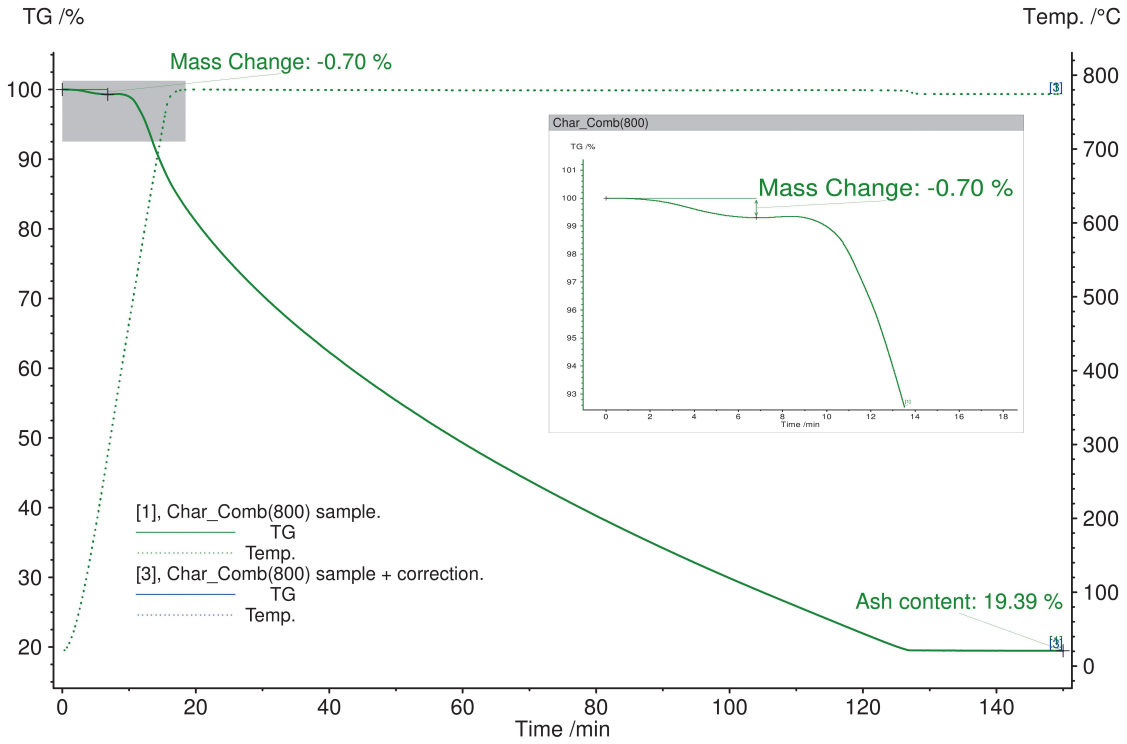

Fig. 3. Combustion of the pyrolysis char in synthetic air (Run No. 3, Table 3). Two overlapping curves are shown: [1] Char_Comb(800) sample – measurement for the sample without correction but in BeFlat®mode, [2] Char_Comb(800) sample + correction – measurement for the sample with correction

Figure 4 shows a comparison of the relative mass gains due to adsorption of acetone for GAC and pyrolysis char. Prior to adsorption, the samples were degassed by increasing temperature up to 200 and 500 °C for the two respective materials. Noticeable mass loss due to desorption of moisture and volatiles (13.4 wt% in total) was observed only for GAC while it was negligibly small (below 1 wt%) for the pyrolysis char.

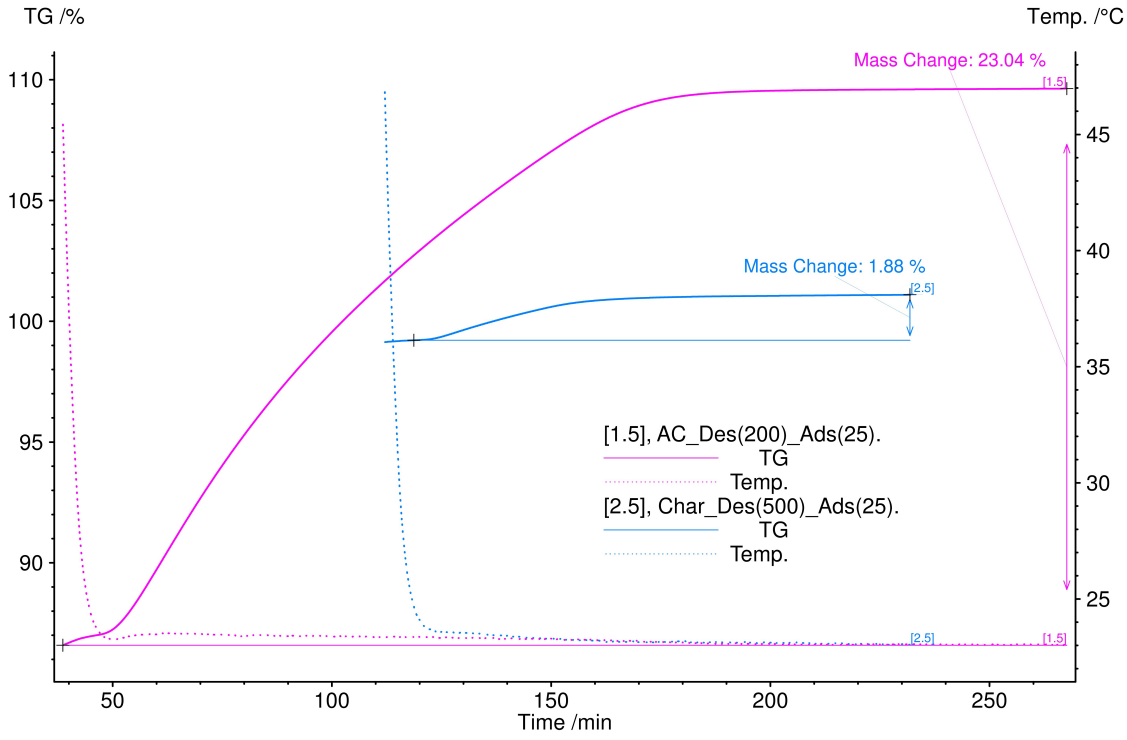

Fig. 4. Adsorption of acetone vapour on GAC and the pyrolysis char (Runs No. 1 and 2, Table 3)

Adsorption started immediately after introducing acetone vapour in the vicinity of adsorbent. When equilibration was reached, the mass gain for GAC and the pyrolysis char was 23.04 and 1.88 wt%, respectively. These values were recalculated to the equilibrium adsorption capacity using the following equation

$$q_e = \frac{\Delta m_{r,ads}}{m_{r,ini}} 100\% \tag{1}$$

where: $\Delta m_{r,ads}$ is the relative mass gain due to adsorption of acetone, and $m_{r,ini}$ is the relative mass of adsorbent before adsorption. Finally, the following equilibrium adsorption capacities were obtained: 266.1 and 18.9 mg/g for GAC and the pyrolysis char, respectively.

Figure 5 presents the relative mass gains due to adsorption of acetone vapour on the pyrolysis chars activated at different temperatures (see Table 3). For comparison purposes, the relative mass change for the non-activated pyrolysis char is also given. Physical activation using carbon dioxide was performed in two steps. Firstly, the temperature was increased up to the desired temperature. Secondly, the temperature was stabilised for 85 min in the isothermal step. Activation was finished by switching the gas atmosphere from carbon dioxide to nitrogen. Then, the activated char samples were cooled to 25 °C and acetone vapour was introduced to the thermobalance chamber. Mass gain was observed during adsorption. The measurement was completed after the mass gain stabilised.

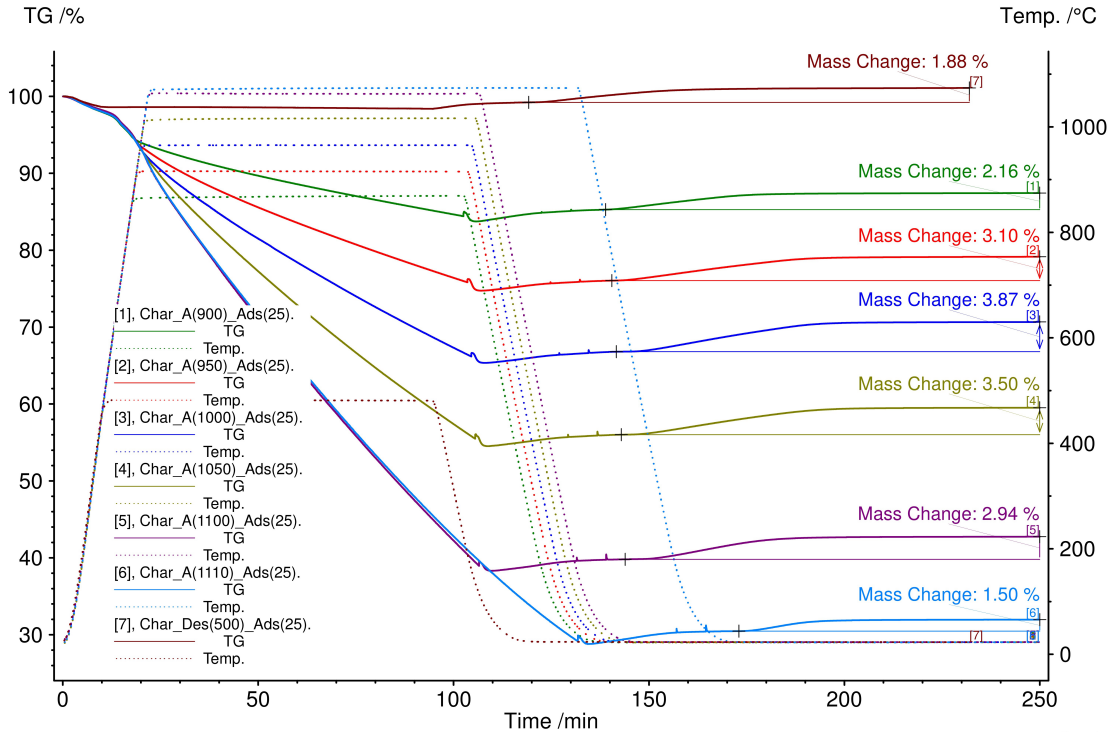

Fig. 5. Activation of pyrolysis chars followed by adsorption of acetone vapour (Runs No. 2 and 4–9, Table 3)

Activation of pyrolysis char using carbon dioxide refers to the following Boudouard reaction

$$C + CO_2 \leftrightarrow 2CO \tag{2}$$

The carbon burn-off is clearly related to the activation temperature and time (Fig. 5). The calculated burn-offs for all performed measurements are listed in Table 4. Note that two effects can be observed when the activation temperature increases: 1) decreasing yield, and 2) development of the porous structure of activated char (Table 5). Both effects refer directly to the burn-off. The former is decisive up to a certain optimum burn-off while the latter is crucial after exceeding this optimum. In other words, when the contribution of mineral part in activated char is too high, the equilibrium adsorption capacity drops (see Table 4).

Table 4. Characteristics of measurements carried out for the non-activated and activated pyrolysis chars

Run No.	Measurement name	Yield (%)	Burn-off (%)	Relative mass change due to adsorption of acetone (%)	Equilibrium adsorption capacity (mg/g)
2	Char_Des(500)_Ads(25)	–	–	1.88	18.9
4	Char_A(900)_Ads(25)	84.42	14.98	2.16	25.3
5	Char_A(950)_Ads(25)	75.83	23.64	3.10	40.8
6	Char_A(1000)_Ads(25)	66.31	33.22	3.87	57.9
7	Char_A(1050)_Ads(25)	55.59	44.02	3.50	62.5
8	Char_A(1100)_Ads(25)	39.08	60.64	2.94	73.9
9	Char_A(1110)_Ads(25)	29.17	70.62	1.50	17.6

Figure 6 presents performance of the char activated at 1000 °C which was subjected to eleven subsequent adsorption/desorption cycles. A slight deterioration of the equilibrium adsorption capacity with increasing number of cycles is clearly visible. The equilibrium adsorption capacity decreases from 60.2 mg/g for the first cycle to 53.8 mg/g for the last cycle, i.e. about 10%.

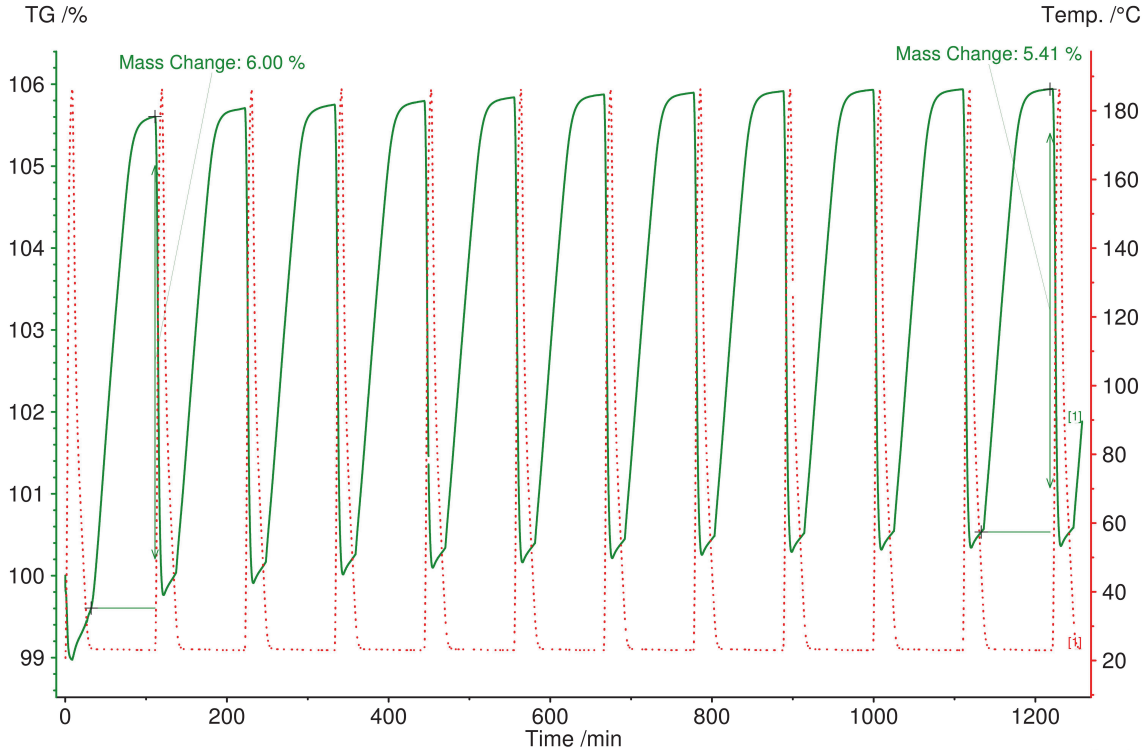

Fig. 6. Adsorption/desorption cycles carried out for the char activated at 1000 °C (Run No. 10, Table 3)

Figure 7 shows a comparison of the nitrogen adsorption isotherms for GAC as well as the non-activated and activated pyrolysis chars. Clearly, GAC adsorption isotherm is composite of type I and type IV. The initial reversible filling of micropores (< 2 nm) is followed by multilayer adsorption and capillary condensation taking place in mesopores (2–50 nm). The observed plateau indicates complete mesopore filling. On the other hand, the non-activated and activated pyrolysis chars are type II isotherms. In this case, the pore condensation also occurs in large meso- and macropores, which is seen as a sharp increase of the

adsorbed amount close to the saturation pressure. The hysteresis loops are also different for GAC and the non-activated and activated pyrolysis chars. The type H4 hysteresis loop has been identified for GAC, while the type H3 hysteresis loop has been linked to the non-activated and activated chars. However, both hysteresis loops have the typical steep region of the desorption branches closing the hysteresis loops at $P/P^o \sim 0.42$. This is characteristic for the nitrogen hysteresis loops. Note that the slit-like pores are associated with the H3 and H4 loops.

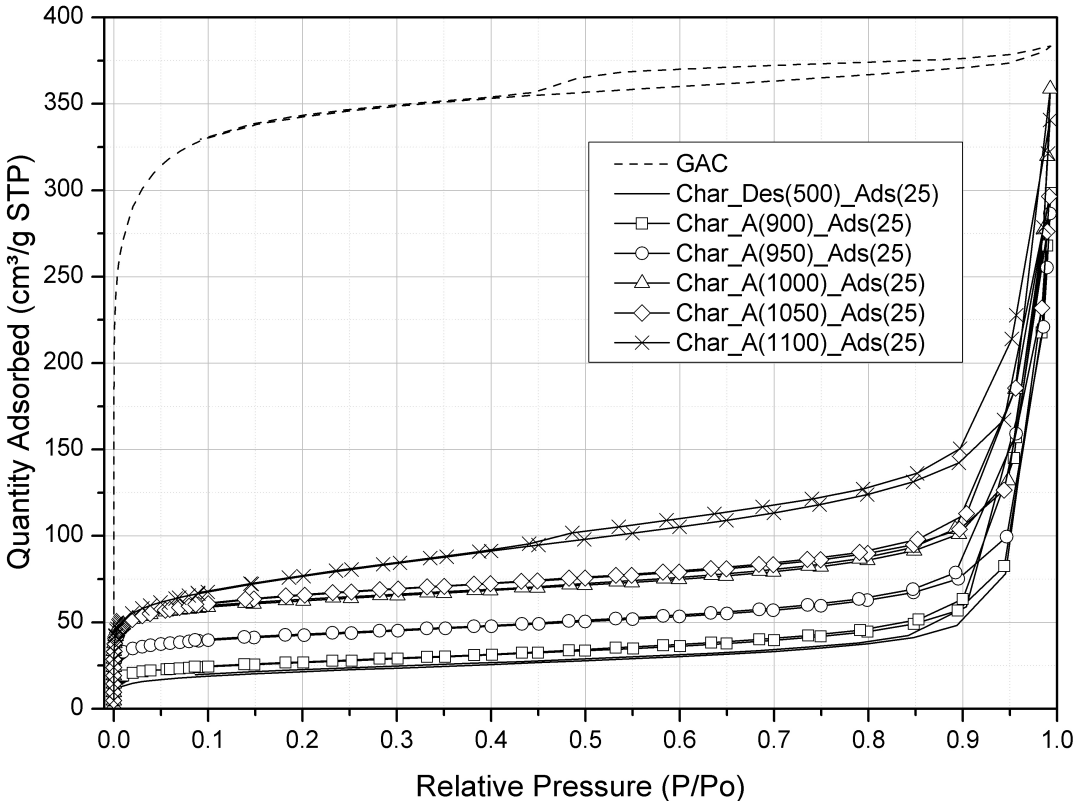

Fig. 7. Nitrogen adsorption/desorption isotherms for GAC and the non-activated and activated chars at 77 K

Since the H3 hysteresis loop does not have a plateau at high relative pressures, the pore size distribution in the mesopore range cannot be evaluated using classical methods based on the modified Kelvin equation, such as the Barrett–Joyner–Halenda (BJH) method. Instead, microscopic methods using statistical mechanics, such as the NLDFT or Grand Canonical Monte Carlo, can be applied. Using these methods, an accurate pore size analysis over the complete micro- and mesopore size range is possible.

Figure 8 shows a comparison of the pore size distributions for all tested activated pyrolysis chars. The distributions cover a wide range of the pore sizes from micropore up to the meso-macropore range ($>$ 50 nm). There are clear differences between the displayed pore size distributions. When the activation temperature increases, the activated pyrolysis chars tend to develop their microporous structure at the expense of their mesoporosity. This observation is also reflected in the shapes of nitrogen adsorption isotherms (Fig. 7) which display progressive uptake of nitrogen in the micropore range with the increasing activation temperature. The development of the microporous structure is very beneficial for the adsorption of small molecules with the critical diameters in the microporous range ($<$ 2 nm). Then, they can easily enter the micropores. Note that the critical diameter of acetone molecule is about 0.48 nm.

Figure 9 shows a comparison of the pore size distributions for three samples: GAC, non-activated char and activated char at 1100 °C. Note that GAC and the non-activated char represent two limiting cases, in which pores are practically microporous and mesoporous, respectively. On the other hand, the activated pyrolysis char has an intermediate internal structure with pores present in the two ranges.

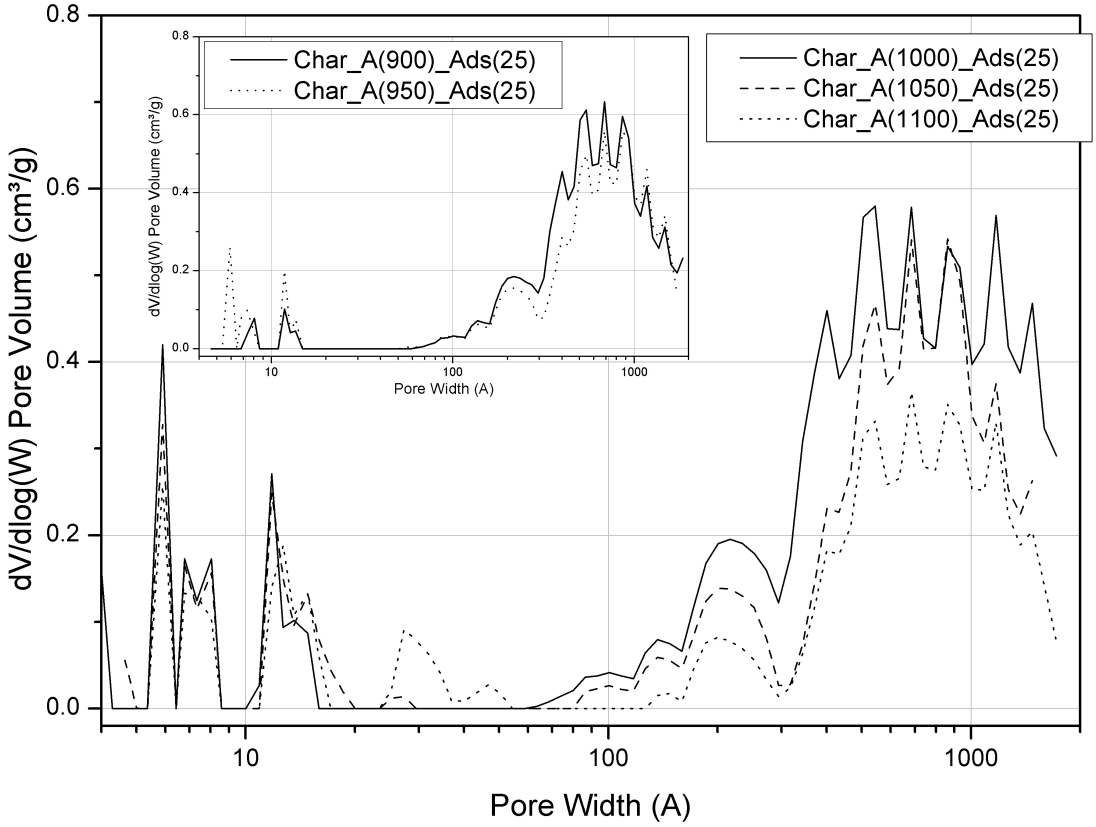

Fig. 8. Pore size distributions for the activated pyrolysis chars at different temperatures. The distributions calculated with the N2-DFT model

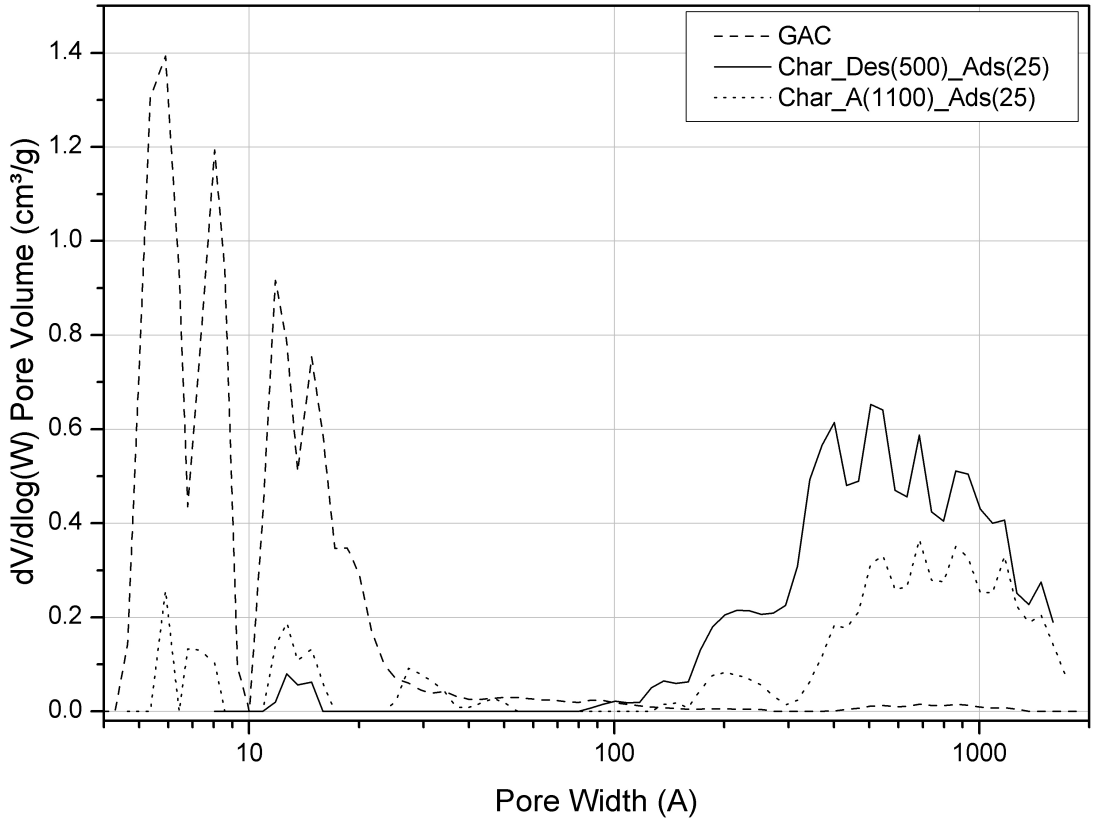

Fig. 9. Pore size distributions for GAC and the pyrolysis chars: non-activated and activated at 1100 °C. The distributions calculated with the N2-DFT model

The goodness of fit of the N2-DFT model predictions to the experimental adsorption isotherms is very good as detailed in Fig. A1 (see Appendix). This indicates that the chosen model is appropriate.

Table 5 details the data on BET surface area, t-plot micropore area and total volume in pores for all performed experiments.

Table 5. Textural properties of GAC and the non-activated and activated char

Run No.	Sample name	BET surface area (m^2/g)	t-Plot micropore area (m^2/g)	DFT	
				Pore size (Å)	Total volume in pores (cm^3/g)
1	GAC	1333.5161	1082.0701	$\leq$ 1858.04	0.47295
2	Char_Des(500)_Ads(25)	76.2973	18.2945	$\leq$ 1593.55	0.40049
4	Char_A(900)_Ads(25)	96.8110	41.3177	$\leq$ 1858.04	0.39552
5	Char_A(950)_Ads(25)	157.9748	91.9604	$\leq$ 1720.79	0.35329
6	Char_A(1000)_Ads(25)	235.9439	157.0492	$\leq$ 1720.79	0.44940
7	Char_A(1050)_Ads(25)	242.6062	133.4848	$\leq$ 1475.96	0.32750
8	Char_A(1100)_Ads(25)	271.7532	73.2446	$\leq$ 1720.79	0.25227
9	Char_A(1000)_CyclesAdsDes	205.3731	123.4417	$\leq$ 1720.79	0.46997

4. CONCLUSIONS

TGA has proved to be a very efficient method for investigating physical activation of TPCs. In addition, the introduction of acetone vapour (a typical representative of volatile organic compounds) into the thermobalance has extended the possibility of testing for vapour adsorption on TPC.

There are two important effects associated with the activation of TPC: (1) decreasing yield, i.e. decreasing mass of TPC due to the activation, and (2) development of the char's porous structure. Both effects result from the carbon burn-off (the Boudouard reaction). The calculated equilibrium adsorption capacity increases with the increasing burn-off only to a certain level. When an optimum burn-off is exceeded, the equilibrium adsorption capacity falls. For the tested TPC, the optimum burn-off can be estimated in the range between 60 and 70%. The equilibrium adsorption capacity of the activated TPC decreases by about 10% after eleven adsorption/desorption cycles.

The surface characterisation studies reveal that the porous structure of TPCs changes as a result of the physical activation with carbon dioxide. In general, the original mesoporous structure of the non-activated pyrolysis char is shifted towards microporous structure for the activated pyrolysis chars. Although the BET surface area increases with increasing burn-off, the micropore area decreases when the burn-off is higher than $\sim$ 33%.

SYMBOLS

m sample mass, mg
q_e equilibrium adsorption capacity, mg/g

Temp temperature, °C
TG relative sample mass, %
V volume, cm^3
W pore width, Å

Subscripts

ads adsorption
ini initial
r relative

The project funded by the National Centre for Research and Development and the European nion under the European Regional Development Fund under the agreement UOD-DEM-1-217/001.

REFERENCES

Acevedo B., Barriocanal C., 2015. Texture and surface chemistry of activated carbons obtained from tyre wastes. *Fuel Process. Technol.*, 134, 275–283. DOI: 10.1016/j.fuproc.2015.02.009.

Acosta R., Fierro V., Martinez de Yuso A., Nabarlatz D., Celzard A., 2016. Tetracycline adsorption onto activated carbons produced by KOH activation of tyre pyrolysis char. *Chemosphere*, 149, 168–176. DOI: 10.1016/j.chemosphere.2016.01.093.

Acosta R., Nabarlatz D., Sanchez-Sanchez A., Jagiello J., Gadonneix P., Celzard A., Fierro V., 2018. Adsorption of Bisphenol A on KOH-activated tyre pyrolysis char. *J. Environ. Chem. Eng.*, 6, 823–833. DOI: 10.1016/j.jece.2018.01.002.

Antoniou N., Stavropoulos G., Zabaniotou A., 2014. Activation of end of life tyres pyrolytic char for enhancing viability of pyrolysis – Critical review, analysis and recommendations for a hybrid dual system. *Renew. Sustain. Energy Rev.*, 39, 1053–1073. DOI: 10.1016/j.rser.2014.07.143.

Antoniou N., Zabaniotou A., 2015. Experimental proof of concept for a sustainable End of Life Tyres pyrolysis with energy and porous materials production. *J. Clean. Prod.*, 101, 1–14. DOI: 10.1016/j.jclepro.2015.03.101.

Antoniou N., Zabaniotou A., 2018. Re-designing a viable ELTs depolymerization in circular economy: Pyrolysis prototype demonstration at TRL 7, with energy optimization and carbonaceous materials production. *J. Clean. Prod.*, 174, 74–86. DOI: 10.1016/j.jclepro.2017.10.319.

Cortés F.B., Chejne F., Carrasco-Marín F., Moreno-Castilla C., Pérez-Cadenas A.F., 2010. Water adsorption on zeolite 13X: comparison of the two methods based on mass spectrometry and thermogravimetry. *Adsorption*, 16, 141–146. DOI: 10.1007/s10450-010-9206-5.

ETRMA, 2015. End-of-life *Tyre Report* 2015 36.

Farooq M.Z., Zeeshan M., Iqbal S., Ahmed N., Shah S.A.Y., 2018. Influence of waste tire addition on wheat straw pyrolysis yield and oil quality. *Energy*, 144, 200–206. DOI: 10.1016/j.energy.2017.12.026.

Hadi P., Yeung K.Y., Guo J., Wang H., McKay G., 2016. Sustainable development of tyre char-based activated carbons with different textural properties for value-added applications. *J. Environ. Manage.*, 170, 1–7. DOI: 10.1016/j.jenvman.2016.01.005.

Han J., Li W., Liu D., Qin L., Chen W., Xing F., 2018. Pyrolysis characteristic and mechanism of waste tyre: A thermogravimetry-mass spectrometry analysis. *J. Anal. Appl. Pyrolysis*, 129, 1–5. DOI: 10.1016/j.jaap.2017.12.016.

Kruk M., Jaroniec M., Guan S., Inagaki S., 2001. Adsorption and thermogravimetric characterization of mesoporous materials with uniform organic-inorganic frameworks. *J. Phys. Chem. B*, 105, 681–689. DOI: 10.1021/jp003133f.

Lin H.-Y., Yuan C.-S., Chen W.-C., Hung C.-H., 2006. Determination of the adsorption isotherm of vapour-phase mercury chloride on powdered activated carbon using thermogravimetric analysis. *J. Air Waste Manag. Assoc.*, 56, 1550–1557. DOI: 10.1080/10473289.2006.10464561.

Majchrzak-Kucęba I., Nowak W., 2005. A thermogravimetric study of the adsorption of CO_2 on zeolites synthesized from fly ash. *Thermochim. Acta*, 437, 67–74. DOI: 10.1016/j.tca.2005.06.003.

Martínez J.D., Puy N., Murillo R., García T., Navarro M.V., Mastral A.M., 2013. Waste tyre pyrolysis – A review. *Renew. Sustain. Energy Rev.*, 23, 179–213. DOI: 10.1016/j.rser.2013.02.038.

Muller J.C.M., Hakvoort G., Jansen J.C., 1998. DSC and TG study of water adsorption and desorption on zeolite NaA: Powder and attached as layer on metal. *J. Therm. Anal. Calorim.*, 53, 449–466. DOI: 10.1023/A:1010137307816.

Seng-eiad S., Jitkarnka S., 2016. Untreated and HNO3-treated pyrolysis char as catalysts for pyrolysis of waste tire: In-depth analysis of tire-derived products and char characterization. *J. Anal. Appl. Pyrolysis*, 122, 151–159. DOI: 10.1016/j.jaap.2016.10.004.

Sharma V.K., Mincarini M., Fortuna F., Cognini F., Cornacchia G., 1998. Disposal of waste tyres for energy recovery and safe environment – Review. *Energy Convers. Manage.*, 39, 511–528. DOI: 10.1016/S0196-8904(97)00044-7.

Williams P.T., 2013. Pyrolysis of waste tyres: A review. *Waste Manage.*, 33, 1714–28. DOI: 10.1016/j.wasman.2013.05.003.

Received 06 April 2018
Received in revised form 27 May 2018
Accepted 28 May 2018

APPENDIX

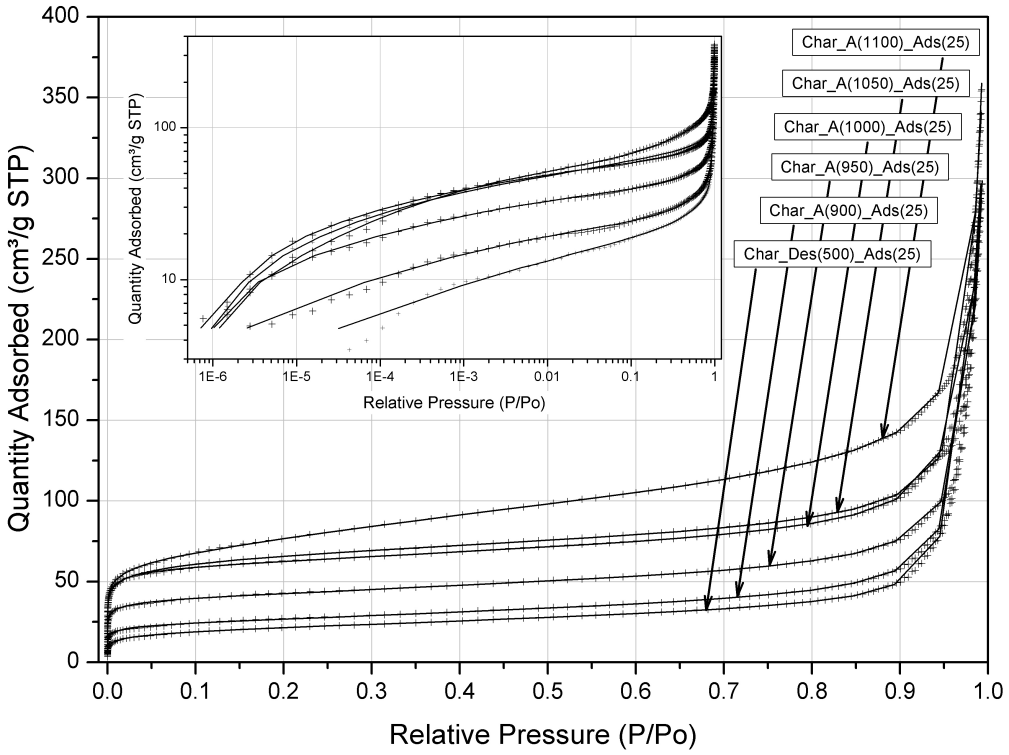

Fig. A1. Goodness of fit of the N2-DFT model to the experimental adsorption isotherms. Standard 1 deviations of fits: 1.18293 cm^3/g STP for Char_A(900)_Ads(25), 1.04269 cm^3/g STP for 2 Char_A(950)_Ads(25), 1.21973 cm^3/g STP for Char_A(1000)_Ads(25), 0.94767 cm^3/g STP for 3 Char_A(1050)_Ads(25), 0.75197 cm cm^3/g STP for Char_A(1100)_Ads(25), 1.26913 cm^3/g STP for 4 Char_Des(500)_Ads(25)